

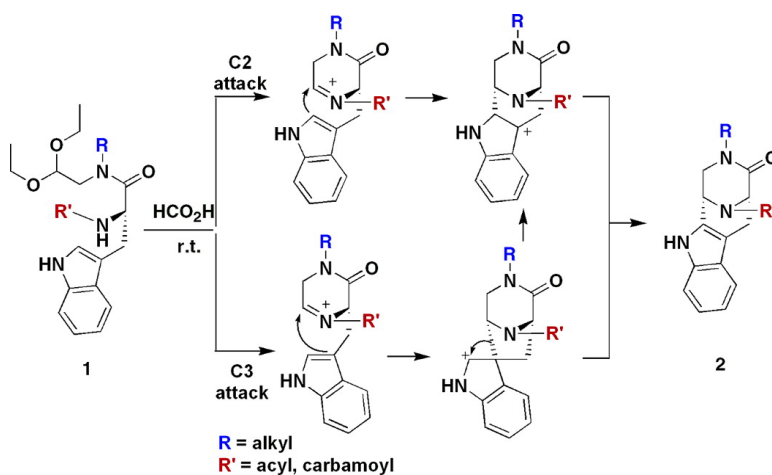
Article

Solid-Phase Parallel Synthesis of Natural Product-Like Diaza-Bridged Heterocycles through Pictet–Spengler Intramolecular Cyclization

Sung-Chan Lee, and Seung Bum Park

J. Comb. Chem., 2006, 8 (1), 50-57 • DOI: 10.1021/cc0501054 • Publication Date (Web): 09 November 2005

Downloaded from <http://pubs.acs.org> on March 22, 2009



More About This Article

Additional resources and features associated with this article are available within the HTML version:

- Supporting Information
- Links to the 4 articles that cite this article, as of the time of this article download
- Access to high resolution figures
- Links to articles and content related to this article
- Copyright permission to reproduce figures and/or text from this article

[View the Full Text HTML](#)

Solid-Phase Parallel Synthesis of Natural Product-Like Diaza-Bridged Heterocycles through Pictet–Spengler Intramolecular Cyclization

Sung-Chan Lee and Seung Bum Park*

School of Chemistry, Seoul National University, Seoul, 151-742, Korea

Received August 14, 2005

A multistep, practical solid-phase strategy for the synthesis of natural product-like diaza-bridged heterocycles was developed. A key step in the library synthesis is tandem acidolytic cleavage with subsequent in situ iminium formation followed by the Pictet–Spengler intramolecular cyclization. The Pictet–Spengler-type intramolecular cyclization step was regioselective and diastereoselective to give final products as single diastereomers in exceptional yields and purities, which was confirmed by NMR structural study and LC/MS analysis. This approach is exemplified by the preparation of a 384-member library of 3,9-diazabicyclo[3.3.1]non-6-en-2-one skeletons, fused with indole and dihydroxybenzene and diversified at two bridging nitrogen atoms, using the solid-phase parallel synthetic methodology without further purification. In this pilot library, two diastereomerically enriched diaza-bridged core skeletons were modified by amide and urea bond formation on bridging nitrogen atoms, and this scheme exhibits the potential for expansion to obtain further diversification.

Introduction

Combinatorial chemistry has transformed into an essential tool for various research disciplines, such as chemical biology and drug discovery.^{1,2} Collections of small organic molecules derived through combinatorial chemistry that specifically perturb the individual function of gene products are facilitating biological pathway explorations in cells or organisms;¹ therefore, the access to libraries of “natural product-like” small molecules is an immediate requirement and a key element in chemical biology.³

The small molecules used most successfully in medicine and biological research have been natural products, which are extremely diverse and often complex;^{4,5} however, unnatural small molecules easily attainable through synthetic exercises have attracted the attention of the scientific community. This is because researchers have experienced difficult hit-to-lead optimization after the identification of initial hits from natural product collections against various therapeutic targets, which is one of the major hindrances in drug discovery. However, productive biological activities involving natural products can be used advantageously by mimicking the key structural motifs of bioactive natural products during the design of synthetic natural product-like small-molecule scaffolds.

To identify new target scaffolds, the pool of diverse natural products was tapped. Hence, various bioactive natural products were scanned, and interesting core scaffolds were extracted for combinatorial construction of a small-molecule library. Ecteinascidins are a family of marine-derived tetrahydroisoquinoline alkaloids that possess an extremely potent antitumor activity.^{6–8} One such marine alkaloid, Yondelis (ET-743), was granted orphan drug status in 2005 in the U.S. and E.U. by the FDA for the treatment of ovarian cancer. Myers and Lanman⁹ reported an extremely refined

solid-phase synthesis of a small series of analogues of (–)-Saframycin A. In addition, several indole alkaloids¹⁰ have been isolated and identified as similar cyclic ring systems; however, their natural scarcity and the complexity of the abovementioned synthetic methods have limited their development as antitumor drugs. Therefore, we focused on the construction of a natural product-like small-molecule library embedded with a common diaza-bridged cyclic structural motif that may induce various biological activities. Toward this goal, solid-phase combinatorial synthesis techniques were implemented for the development of novel reaction pathways to obtain the structural motif while maintaining a complete control of regio- and diastereoselectivity. This is essential for the construction of high-purity small molecule libraries suitable for immediate biological evaluation without further purification, thereby bypassing the chromatographic problem.

Our laboratory is primarily interested in the identification of bioactive small molecules; therefore, an attractive approach is the exploration of the wide variety of biological activities by the collection of diverse small organic molecules through the creative recombination of privileged moieties, such as diazaheterocycles, tryptophan, and DOPA. In this report, we describe a facile access to natural product-like diaza-bridged cyclic templates through efficient Pictet–Spengler intramolecular cyclization with indole and the dihydroxyphenyl group. Several reports are available on the solid-phase Pictet–Spengler reaction, in which aldehydes in solution are condensed with tryptophan on a solid support by *N*-acyliminium formation.¹¹ In addition, the previously reported synthesis of the 3,9-diazabicyclo[3.3.1]non-6-en-2-one core skeleton by Pictet–Spengler intramolecular cyclization consisted of the prior formation of the core skeleton, followed by modification of the bridging nitrogen atom at the 9 position.¹² However, major disadvantages of

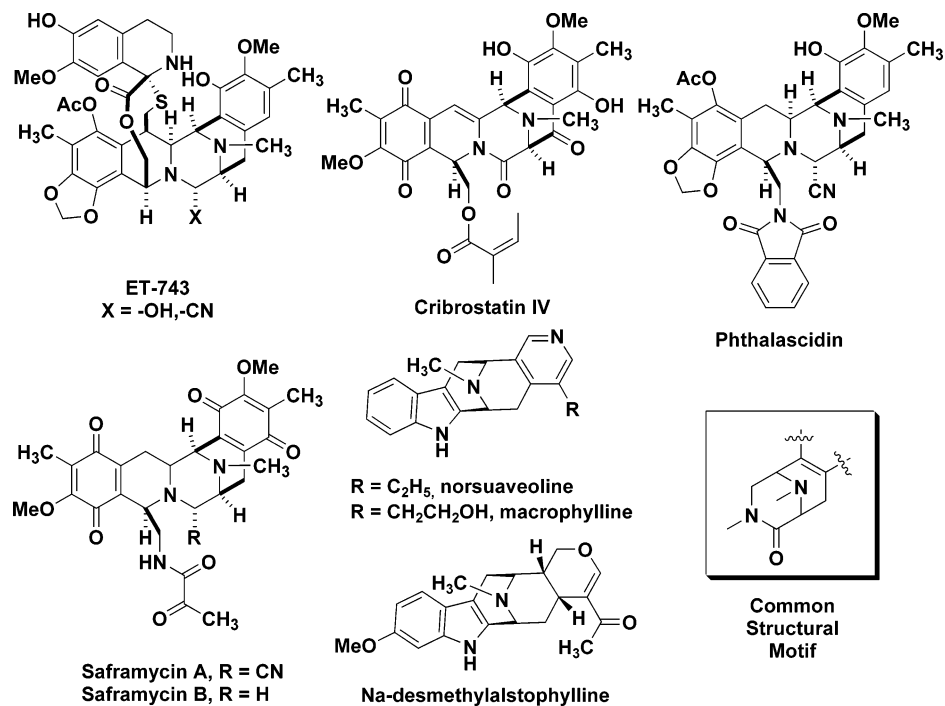


Figure 1. Bioactive natural products with a common diaza-bridged structural motif.

these approaches are the poor diastereoselectivity in the cyclization process, which is a critical limitation during library construction, and the failed application of DOPA moiety for Pictet–Spengler intramolecular cyclization. According to some outstanding reports, the diastereoselective Pictet–Spengler reaction was successfully applied into the combinatorial library construction; however, most approaches dealt with purification steps.¹³ In this report, a novel diastereoselective route for obtaining privileged heterocyclic core skeletons through Pictet–Spengler intramolecular cyclization via acidolytic cleavage/in situ iminium formation was validated. The solid-phase synthesis of a 384-membered pilot library with four different core scaffolds in high purities was carried out without further purification as a single diastereoisomer. The route described in this report also provides facile access to the diversification at two bridging nitrogen atoms at the 3 and 9 positions, which exhibits the potential for expansion to obtain further diversification using solid-phase synthesis.

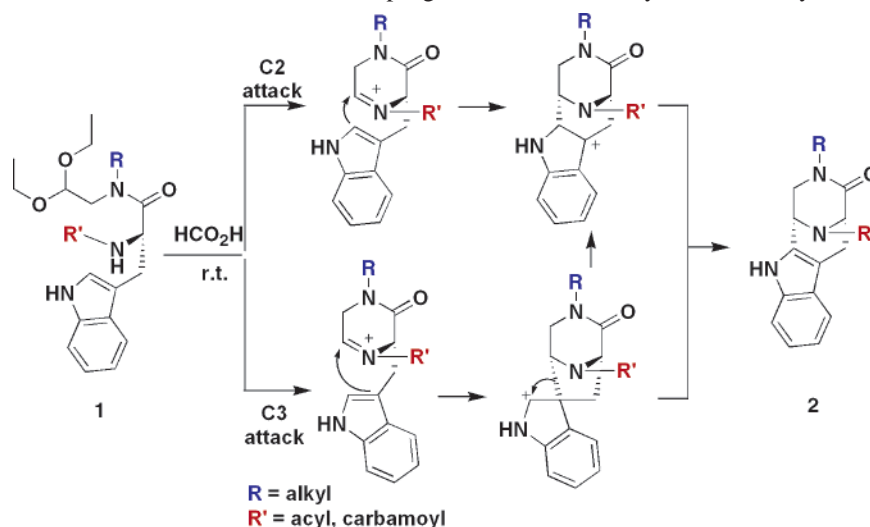
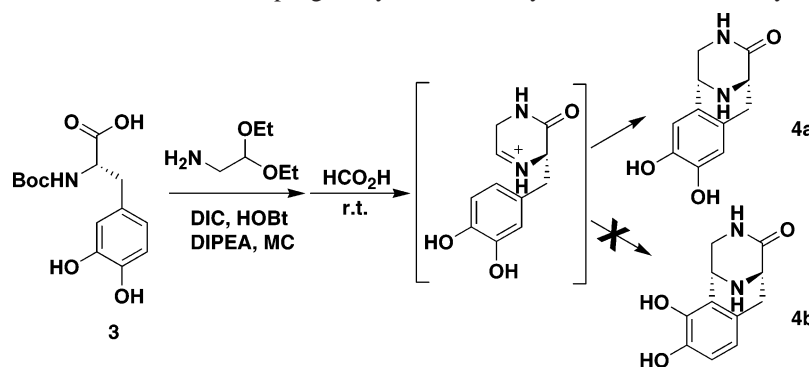
Results and Discussion

While preparing for parallel solid-phase combinatorial synthesis, it is essential that the synthetic procedures are simplified and optimized to produce high yields of diastereomerically enriched small molecules. The Pictet–Spengler-type carbon nucleophiles in indole and the dihydroxyphenyl group can easily attack activated acyliminium intermediates in the presence of acid catalysts. This is a well-known reaction that has been demonstrated as a useful transformation in library construction.¹⁴

Initially, the synthetic procedure was developed and exemplified by the preparation of a representative tryptophan-derived azacycle **2** and the corresponding L-DOPA-derived azacycle **4a**, as shown in Schemes 1 and 2. The regio- and diastereoselectivity of individual transformations, previously

reported by several groups,^{15,16} was confirmed by NMR study of the representative compounds **4a** and **16**{*10,1*} (see Supporting Information). When indoles underwent Pictet–Spengler-type cyclization with various iminium moieties that were generated in situ from masked aldehyde and amide nitrogen under acidic conditions, two modes of nucleophilic attack at carbon positions C2 and C3 in indole (Scheme 1)¹⁷ became possible. C2 attack can afford the formation of a 3,9-diazabicyclo[3.3.1]non-6-en-2-one derivative **2** as a single diastereoisomer. In the case of C3 attack, it was speculated that a spiro-five-membered intermediate was generated, followed by cationic migration and hydride elimination, because **2** was a single regio- and diastereoisomer in this reaction. Compared to our observation, Pátek reported the opposite outcome; diastereoselective Pictet–Spengler intramolecular cyclization by C2 attack.¹⁸ The cyclization condition was also optimized by using various acid sources, such as TFA, PPTS, and formic acid. In addition, the temperature and solvent (data not shown) were also varied. The treatment using neat formic acid accomplished the formation of the desired scaffold in nearly quantitative yields as a single diastereoisomer. This occurred by means of a sequential process of acetal deprotection (acidolytic cleavage in solid-phase synthesis) and in situ cyclic iminium formation followed by intramolecular Pictet–Spengler cyclization. Subsequent functional group compatibility in the intramolecular cyclization was performed to validate the efficient cyclic iminium formation with nitrogen atoms of various functional moieties, such as amide and urea, which were converted into the desired 3,9-diazabicyclo[3.3.1]non-6-en-2-one core structures under optimized acidic conditions.

To diversify the diaza-bridged core skeletons, the Pictet–Spengler-type intramolecular cyclization was applied with a DOPA moiety, which is also an attractive, privileged scaffold and bears nucleophilic carbon centers on an aryl

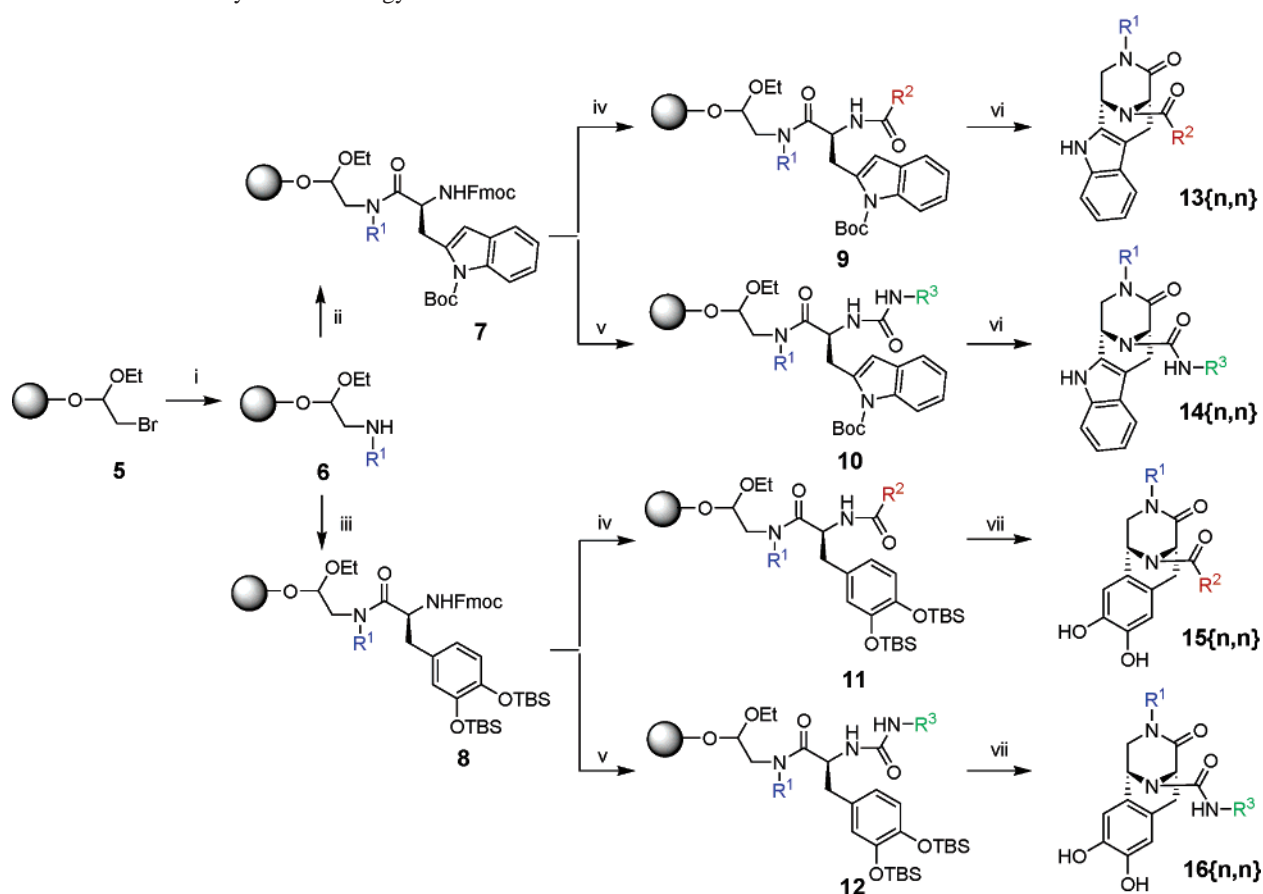
Scheme 1. Regioselective and Diastereoselective Pictet–Spengler Intramolecular Cyclization of Cyclic Iminium with Indole**Scheme 2.** Regio- and Diastereoselective Pictet–Spengler Cyclization of Cyclic Iminium with Dihydroxyphenyl Nucleophile

group. The simplified system using the dihydroxyphenyl group and aminoacetal, as shown in Scheme 2, was utilized to identify the optimum reaction condition and validate the regio- and diastereoselectivity of the final intramolecular cyclization step. There are two possible regioisomers; however, under the optimized condition using DOPA, a single diastereoisomer **4a** was identified and confirmed by ^1H and COSY NMR analysis. To confirm the relative configuration with *N*-substituted DOPA-derived diaza-bridged heterocyclic core structures, extensive NMR studies, including ^1H COSY, NOSEY, HSQC, and HMBC experiments, were pursued with the compound **16**{10,1}. These two critical supporting data revealed that the optimized reaction condition yielded a single diastereoisomer. The exceptional diastereoselectivity of the new chiral center generated by Pictet–Spengler intramolecular cyclization was rationalized by cheminformatics calculation using Insight2000 of Accelrys. There are two possible modes of nucleophilic attack on in situ generated cyclic iminium: *si* face and *re* face. However, the predefined stereochemistry of the α carbon of *L*-amino acids (DOPA or tryptophan) significantly influenced the stereochemical outcome of diaza-bridged heterocycles, which favors an *re* face attack because of the distance between the nucleophilic carbon and the cyclic iminium (see Supporting Information for details).

After the confirmation of regio- and diastereoselective cyclization of indole and dihydroxyphenyl moieties in solution, the solid-phase synthesis of the 3,9-diazabicyclo-

[3.3.1]non-6-en-2-one core skeletons was initiated. Bromoacetal resin was used with the expectation that intramolecular Pictet–Spengler cyclization would occur during the cleavage step under acidic conditions (Scheme 3).¹⁸ The final cleavage/cyclization step successfully provided the desired diaza-bridged templates in high yields and purities without any nonvolatile side products; high-efficiency library construction was therefore ensured. In addition to increasing the number and structural variety of building blocks, our heterocycle library furnished four regio- and diastereochemically distinct core skeletons. In brief, two diastereomerically enriched diaza-bridged templates with indole and DOPA were diversified by introducing various functional moieties on aza-bridging nitrogen atoms. In this pilot library synthesis, we only focused on amide and urea. To visualize the value of diverse skeletons in a single library, identical building blocks were utilized for realization of the library, and the effects of different core skeletons were studied using cheminformatics tools (detailed below).

Prior to the library synthesis, each core structure was validated on a solid support by synthesizing the representative compounds **13**{10,1} and **14**{10,1} ($R^1 = \text{Bn}$, $R^2 = \text{methyl}$), and **15**{10,1} and **16**{10,1} ($R^1 = \text{Bn}$, $R^3 = \text{Bn}$) using bromoacetal resin (**5**). With this confirmation, the possible diversity in space of these templates was explored in parallel synthesis. The library synthesis was initiated by the incorporation of a diversity element through simple amination with bromoacetal resin in a DMSO solution at 60 °C.¹⁸ The

Scheme 3. Solid-Phase Synthetic Strategy^a

^a Reagents and conditions are as follows: (i) R^1NH_2 , DMSO, 60 °C; (ii) Fmoc(*N*-Boc)TrpOH, HATU, DIPEA, DMF, room temperature (RT); (iii) Fmoc(*O*-Di-TBS)DOPA, HATU, DIPEA, DMF, RT; (iv) (a) 25% piperidine, RT; (b) R^2CO_2H , DIC, HOBT, DIPEA, RT; (v) R^3NCO , DIPEA, DCE, RT; (vi) neat HCO_2H , RT; (vii) neat HCO_2H , 60 °C.

bromoacetal resin used was prepared in our lab from Wang resin (loading level: 1.6 mmol/g) because of the low loading level of commercial bromoacetal resin. Amination was the first reaction carried out on the solid support, and the substrate concentration turned out to be the critical element for high conversion. After extensive studies on substrate concentration for amination, 20 equiv of primary amine was used to generate a secondary amine with high loading. The resin-bound secondary amines (**6**) coupled with various carboxylic acids (R^2COOH) activated by the coupling agent, HATU [*O*-(7-azabenzotriazol-1-yl)-*N,N,N'*-tetramethyluronium PF_6]. The completion of the amidation step was confirmed by conducting a negative chloranil test. To establish diversity in our core skeletons, various types of derivatization of resin-bound secondary amines were tested, such as carbamate and urea formation, reductive amination, alkylation,¹² and sulfonylation;¹¹ however, we decided to focus on amide and urea bond formation for the library realization (Scheme 3). The final step was performed under neat formic acid to synchronize the compound cleavage from the solid support and the Pictet–Spengler-type intramolecular cyclization with in situ-generated cyclic iminium. We could observe the complete conversion of cyclization precursors derived from tryptophan (**9**, **10**) to the desired products at room temperature, probably due to the nucleophilicity of the indole moiety. However, in the case of the DOPA-derived cyclization precursors (**11**, **12**), uncyclized byproducts were

observed when they were treated at room temperature. Therefore, the final cyclization reaction was tested at an elevated temperature of 60 °C, which accomplished complete cyclization for the core skeletons **15** and **16**.

The practical, solid-phase synthesis of diaza-bridged heterocycles was successfully conducted on a platform comprising 96 parallel, deep-well filtration blocks. Table 1 shows the structures of the various building blocks: primary amine (R^1-NH_2), carboxylic acid (R^2-COOH), and isocyanate (R^3-NCO). The diversity of these core skeletons was expanded by the introduction of various R^1 's by using both in-house-synthesized and commercial primary amines to enhance potentials as bioactive perturbagens. For this pilot library, the secondary amines were exposed to only two types of modification, which allows future diversification during the stage of focused library construction. During solid-phase parallel synthesis of this library, 40 mg of high-loading bromoacetal resin (1.6 mmol/g) was used per library member, which yielded 10–20 mg of final products without further purification. After the completion of library construction, an aliquot of the crude reaction was injected onto a LC/MS instrument to determine the identity and purity. In total, 384 diaza-bridged heterocycles with four different core skeletons, chemsets **13**, **14**, **15**, and **16**, were prepared. The purity and identity of all the library members were assessed by direct analysis of the crude product using LC/MS (Table 1). The presence of all desired compounds was unambiguously

Table 1. Sets of Building Blocks and Purities of Chemsets 13, 14, 15, and 16 Synthesized According to Scheme 3

R ¹		R ²		R ³		Purity	
1	2	3	4	5	6	7	8
13(1,1)	15(1,1)	13(2,1)	15(2,1)	13(3,1)	15(3,1)	13(4,1)	15(4,1)
13(1,2)	15(1,2)	13(2,2)	15(2,2)	13(3,2)	15(3,2)	13(4,2)	15(4,2)
13(1,3)	15(1,3)	13(2,3)	15(2,3)	13(3,3)	15(3,3)	13(4,3)	15(4,3)
13(1,4)	15(1,4)	13(2,4)	15(2,4)	13(3,4)	15(3,4)	13(4,4)	15(4,4)
13(1,5)	15(1,5)	13(2,5)	15(2,5)	13(3,5)	15(3,5)	13(4,5)	15(4,5)
13(1,6)	15(1,6)	13(2,6)	15(2,6)	13(3,6)	15(3,6)	13(4,6)	15(4,6)
13(1,7)	15(1,7)	13(2,7)	15(2,7)	13(3,7)	15(3,7)	13(4,7)	15(4,7)
13(1,8)	15(1,8)	13(2,8)	15(2,8)	13(3,8)	15(3,8)	13(4,8)	15(4,8)
14(1,1)	16(1,1)	14(2,1)	16(2,1)	14(3,1)	16(3,1)	14(4,1)	16(4,1)
14(1,2)	16(1,2)	14(2,2)	16(2,2)	14(3,2)	16(3,2)	14(4,2)	16(4,2)
14(1,3)	16(1,3)	14(2,3)	16(2,3)	14(3,3)	16(3,3)	14(4,3)	16(4,3)
14(1,4)	16(1,4)	14(2,4)	16(2,4)	14(3,4)	16(3,4)	14(4,4)	16(4,4)
14(1,5)	16(1,5)	14(2,5)	16(2,5)	14(3,5)	16(3,5)	14(4,5)	16(4,5)
14(1,6)	16(1,6)	14(2,6)	16(2,6)	14(3,6)	16(3,6)	14(4,6)	16(4,6)
14(1,7)	16(1,7)	14(2,7)	16(2,7)	14(3,7)	16(3,7)	14(4,7)	16(4,7)
14(1,8)	16(1,8)	14(2,8)	16(2,8)	14(3,8)	16(3,8)	14(4,8)	16(4,8)

Template	R ¹	R ²	R ³	Purity
				>90%
				80%-90%
				70%-80%
				<70%

^a Purity was determined by RP-HPLC/MS analysis of the final crude products after cleavage from the solid support with neat formic acid.

Table 2. Purities and ESMS of Representative Library Members

ID	R ¹	R ²	R ³	purity (%)	MS [M + H] ⁺	
					calcd	obs
13{2,3}	3-(trifluoromethyl)-benzyl	benzyl		96.7	504.18	504.03
13{4,4}	4-fluorobenzyl	<i>trans</i> -phenylvinyl		96.9	466.20	466.77
15{4,4}	4-fluorobenzyl	<i>trans</i> -phenylvinyl		86.3	459.49	459.87
13{10,8}	benzyl	2-furanyl		95.6	412.16	412.06
15{7,4}	4-methoxyphenethyl	<i>trans</i> -phenylvinyl		99.2	485.55	485.93
14{9,1}	4-methoxybenzyl		benzyl	93.7	481.56	481.09
16{7,1}	4-methoxyphenethyl		benzyl	91.4	488.56	488.85
14{10,2}	benzyl		allyl	95.1	401.19	401.11
16{7,2}	4-methoxyphenethyl		allyl	96.7	438.49	438.88
14{12,4}	2,2-diphenylethyl		<i>n</i> -hexyl	94.6	535.30	535.19
16{12,4}	2,2-diphenylethyl		<i>n</i> -hexyl	88.1	528.66	528.95
16{1,7}	isobutyl		4-chlorophenyl	90.3	430.90	430.82

confirmed by their molecular mass with a purity range of 70–100%, which was determined by HPLC analysis using a PDA detector. The purity of individual compounds is indicated in Table 1 in different colors; Table 2 shows the crude product analysis results for 12 representative library members with complete spectral data (see the Experimental Section). Overall, the average purity of this library was 90%, and more than 95% of the crude library members exhibited an exceptional purity (>85%).

To visualize the skeletal diversity of this library, a skeletal diversity matrix, which included all the members of this library, was developed on the bases of molecular descriptors, such as cLogP, molecular weight, number of hydrogen bonding donors and acceptors, and number of rotatable bonds. Among the molecular descriptors, 38 self-differentiating molecular descriptors were subjected to principal component analysis. The resulting six principal components can

be extracted to represent 90.9% of the overall descriptors. For improving visualization, Figure 2 was constructed with 3 principal components that represent 81.2% of the total diversity. From unbiased calculations using PreADME (BMD, Seoul, Korea) and illustrations using SigmaPlot (Systat Software Inc., Richmond, CA), it was observed that the four skeletally distinct products distributed differently in the three-dimensional chemical space, which emphasized the importance of skeletal diversity.

Conclusion

We have described a practical method for solid-phase synthesis of 3,9-diazabicyclo[3.3.1]non-6-en-2-one core skeletons recombined with privileged indole and DOPA. The key synthetic strategy for this library involved a sequential cyclic iminium formation and Pictet–Spengler cyclization under the acidolytic cleavage condition, which yielded a

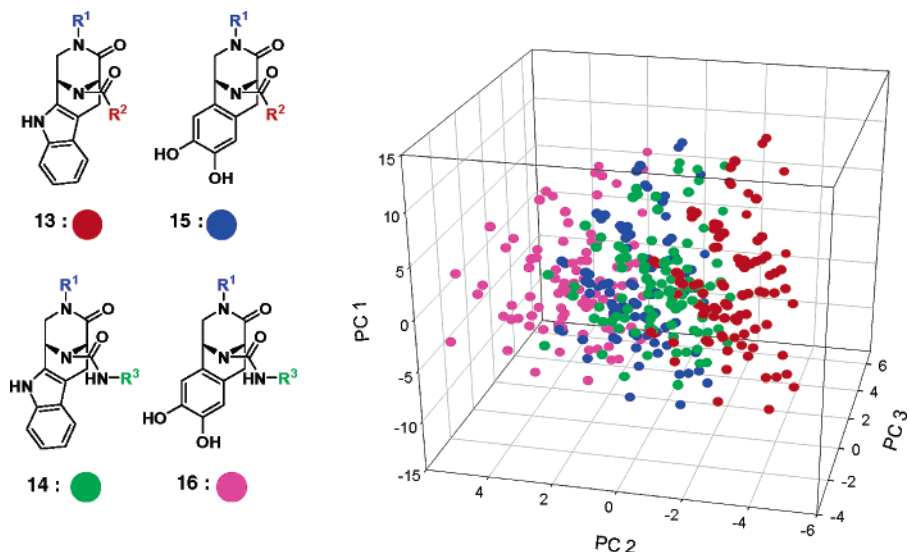


Figure 2. Principal component analysis of chemsets **13**, **14**, **15**, and **16**, differently color-coded for visualization.

diaza-bridged heterocyclic structural motif embedded in various bioactive natural products. This intramolecular reaction proceeds under strict control of regio- and diastereoselectivity, and only a single diastereoisomer is detected in the final crude product. Simplified and highly efficient synthetic protocols were tolerant toward various building blocks, which eliminated the tedious building block rehearsals, and the desired library members were synthesized in parallel with excellent overall yields and purities. Biological evaluations of this small molecule collection are currently underway. These will guide us toward the untouched amine diversification (i.e., alkylation and sulfonylation, etc.) of the focused library construction. The biological results and the focused library construction will be reported in the future.

Experimental Section

General Information. All commercially available reagents and solvents were used without further purification unless mentioned otherwise. All the solvents, such as DMF, methanol, dichloromethane, and DMSO (of HPLC grade), were purchased from Aldrich and Baker. Solution-phase reactions were monitored by analytical thin-layer chromatography (TLC) and purified by preparative TLC performed using an indicated solvent on E. Merck silica gel 60 F₂₅₄ plates (0.25 and 0.5 mm). The compounds were visualized by staining the plate with a cerium sulfate/ammonium molybdate solution; this was followed by heating. Bromoacetal resins were obtained from either Advanced ChemTech or Aldrich, but the high-loading resins for actual library construction were synthesized in our laboratory. The reaction steps for the library construction of the aza-bridged bicyclic templates were performed in parallel using a FlexChem Synthesis System from SciGene (Sunnyvale, CA) consisting of 96 deep-well filtration blocks. The reaction volume per well was set to 1.2 mL unless mentioned otherwise. The purity of all the library members was observed by HPLC/MS spectra, which were recorded on a Water Alliance LC/MS system consisting of a Micromass Quattro micro mass spectrometer, a photodiode array detector, and a 2795 HT-HPLC system equipped with a Waters 120 ODS-BP column

(C-18, 35 × 5 mm, 3 m). NMR spectra were obtained on a Bruker 300-MHz and a Varian INOVA 500-MHz spectrophotometer. Chemical shifts (δ) are quoted in parts per million and referenced to TMS and DMSO-*d*₆.

General Solid-Phase Reaction Procedures. Step 1: Amine Substitution. Bromoacetal resin (40 mg, 1.6 mmol/g, 0.064 mmol) was loaded into each well of a Robbins 96 deep-well filtration block, and solutions of 12 different R¹-amines (20 equiv in DMSO, 1.2 mL) were dispensed into the designated wells of the reaction block. The reaction mixture was shaken at 60 °C in a rotating oven [Robbins Scientific] for 12 h. The resulting resins were washed extensively with DMF, MeOH, and DCM sequentially (three times each) and dried in a high-vacuum desiccator.

Step 2: Amino-Acid Coupling. A reaction cocktail of Fmoc-Trp(Boc)-OH [Senn Chem AG, Switzerland] or Fmoc-L-DOPA(DiTBDS)-OH (3 equiv), HATU (3 equiv), and DIPEA (6 equiv) in DMF (1.2 mL/well) was added to each well that was charged with the resins. The reaction mixture was incubated in a rotating oven for 12 h at room temperature. The resin was then washed extensively with DMF, MeOH, and DCM sequentially (three times each) and dried in a high-vacuum desiccator.

Step 3a: Acid Coupling. Piperidine (25%) in DMF was added to the resins in the reaction block, and the reaction mixture was shaken for 1 h at room temperature. The resins were then washed extensively with DMF, methanol, DCM, and then again with DMF. The active ester was in situ-generated by acid activation (3 equiv) by DIC (3 equiv) and HOBt (3 equiv) in DMF for 30 min. Subsequently, the reaction cocktail was dispensed into the well charged with resins, and the reaction mixture was incubated in a rotating oven for 12 h at room temperature. The resins were washed extensively with DMF, MeOH, and DCM and dried in a high-vacuum desiccator.

Step 3b: Isocyanate Coupling. Piperidine (25%) in DMF was added to the resin in the reaction block, and the reaction mixture was shaken for 1 h at room temperature. The resins were then washed extensively with DMF, MeOH, and DCM. A solution of isocyanate (3 equiv) and DIPEA (3 equiv) in

DCE was dispensed into the well charged with resins, and the reaction mixture was incubated in a rotating oven for 5 h at room temperature. The resins were washed with DMF, MeOH, and then again with DCM and dried in a high-vacuum desiccator.

Step 4: Cleavage and Cyclization. After drying the resins in the 96 deep-well reaction blocks under a high vacuum, the resins were treated with 100% formic acid (1.2 mL/well) for 18 h at room temperature. After removing resins by filtration, the filtrate was condensed in vacuo using a Speedvac (Thermo Savant) to obtain the desired product as a film. The products were diluted with 50% water/acetonitrile and freeze-dried, which yielded a pale yellow powder. The purity of the final products was observed by LC/MS without further purification.

Characterization of Compound 13{10,1}. $^1\text{H NMR}$ (300 MHz, CDCl_3) 7.75 (s, 1H), 7.53 (d, $J = 7.6$, 1H), 7.30–7.16 (m, 4H), 6.85 (t, 2H), 6.57 (d, $J = 7.6$, 2H), 6.00 (d, $J = 3.4$, 1H), 5.00 (d, $J = 15.2$, 1H), 4.92 (d, $J = 5.3$, 1H), 4.07 (d, $J = 14.9$, 1H), 3.79 (dd, $J = 11.9$, 4.2, 1H), 3.45 (d, $J = 5.6$, 1H), 3.23 (m, 2H), 2.22 (s, 3H); MS (ESI $^+$) m/z 360.31 [M + H] $^+$.

Characterization of Compound 14{10,1}. $^1\text{H NMR}$ (300 MHz, CDCl_3) 8.83 (s, 1H), 7.33–6.99 (m, 10H), 6.81 (t, 2H), 6.50 (d, $J = 7.2$, 2H), 6.42 (bt, 1H), 5.67 (d, $J = 3.0$, 1H), 5.07 (d, $J = 3.6$, 1H), 4.64 (d, $J = 15.3$, 1H), 4.27 (t, 2H), 4.02 (d, $J = 15.3$, 1H), 3.69 (dd, $J = 11.8$, 3.8, 1H), 3.12 (m, 3H); MS (ESI $^+$) m/z 451.03 [M + H] $^+$.

Characterization of Compound 15{10,1}. $^1\text{H NMR}$ (300 MHz, $\text{DMSO}-d_6$) 7.13 (m, 3H), 6.73 (m, 2H), 6.66 (s, 1H), 6.51 (s, 1H), 5.69 (d, $J = 3.1$, 1H), 5.32 (s, 1H), 4.79 (m, 2H), 4.26 (m, 1H), 3.56 (dd, $J = 11.9$, 4.2, 1H), 3.18 (m, 3H), 2.15 (s, 3H); MS (ESI $^+$) m/z 352.99 [M + H] $^+$, 375.03 [M + Na] $^+$.

Characterization of Compound 16{10,1}. $^1\text{H NMR}$ (300 MHz, CDCl_3) 7.24 (m, 5H), 7.11 (m, 3H), 6.71 (m, 2H), 6.61 (s, 1H), 6.48 (s, 1H), 6.16 (t, 1H), 5.26 (bs, 1H), 4.94 (d, $J = 5.3$, 1H), 4.72 (d, $J = 15.7$, 1H), 4.39 (d, $J = 5.3$, 2H), 4.20 (d, $J = 5.3$, 1H), 4.56 (dd, $J = 11.9$, 4.2, 1H), 3.18 (m, 1H), 3.01 (m, 2H); MS (ESI $^+$) m/z 444.46 [M + H] $^+$, 466.43 [M + Na] $^+$.

Representative Compounds of Library Members in Table 2. Characterization of Compound 13{2,3}. $^1\text{H NMR}$ (300 MHz, CDCl_3) 8.16 (s, 1H), 7.44–7.08 (m, 11H), 6.75 (t, $J = 7.7$, 1H), 6.78 (d, $J = 7.6$, 1H), 6.06 (d, $J = 3.8$, 1H), 5.01 (d, $J = 5.3$, 1H), 4.86 (d, $J = 15.3$, 1H), 4.16 (d, $J = 15.2$, 1H), 3.83 (d, $J = 6.1$, 2H) 3.79–3.74 (m, 1H), 3.2 (bt, 2H), 2.81 (m, 1H); MS (ESI $^+$) m/z 504.03 [M + H] $^+$.

Characterization of Compound 13{4,4}. $^1\text{H NMR}$ (300 MHz, CDCl_3) 8.21 (s, 1H), 7.77 (d, $J = 15.3$, 1H), 7.58–7.40 (m, 6H), 7.26–7.13 (m, 3H), 6.91 (d, $J = 15.6$, 1H), 6.50 (m, 4H), 6.11 (bs, 1H), 5.21 (d, $J = 5.4$, 1H), 4.96 (d, $J = 15.2$, 1H), 3.69 (d, $J = 15.3$, 1H), 3.83 (dd, $J = 12.4$, 4.2, 1H) 3.45–3.21 (m, 3H); MS (ESI $^+$) m/z 465.80 [M + H] $^+$.

Characterization of Compound 13{10,8}. $^1\text{H NMR}$ (300 MHz, CDCl_3) 8.04 (bs, 1H), 7.51 (m, 2H), 7.27–7.13 (m, 4H), 7.05 (t, $J = 7.3$, 1H), 6.85 (t, $J = 8.0$, 2H), 6.57 (m, 3H), 6.00 (d, $J = 3.4$, 1H), 5.68 (s, 1H), 5.00 (d, $J = 14.8$,

1H), 4.00 (dd, $J = 12.2$, 3.8, 2H), 3.45 (s, 2H), 3.28 (d, $J = 11.8$, 1H); MS (ESI $^+$) m/z 412.03 [M + H] $^+$.

Characterization of Compound 14{9,1}. $^1\text{H NMR}$ (300 MHz, CDCl_3) 8.43 (bs, 1H), 7.39 (d, $J = 6.9$, 1H), 7.26–7.07 (m, 8H), 6.49 (d, $J = 8.8$, 2H), 6.36 (d, $J = 8.8$, 2H), 5.85 (bt, 1H), 5.67 (d, $J = 3.0$, 1H), 4.92 (bs, 1H), 4.72 (d, $J = 14.9$, 1H), 4.36 (d, $J = 4.9$, 2H), 4.00 (d, $J = 14.8$, 1H), 3.74 (dd, $J = 11.8$, 3.4, 1H), 3.63 (s, 3H), 3.19 (m, 3H); MS (ESI $^+$) m/z 481.09 [M + H] $^+$.

Characterization of Compound 14{10,2}. $^1\text{H NMR}$ (300 MHz, CDCl_3) 8.59 (s, 1H), 7.37 (d, $J = 7.2$, 1H), 7.16–7.07 (m, 4H), 6.86 (t, $J = 7.6$, 2H), 6.60 (d, $J = 7.2$, 2H), 5.84 (m, 1H), 5.71 (d, $J = 3.5$, 1H), 5.63 (t, $J = 5.7$, 1H), 5.16–4.98 (m, 3H), 4.80 (d, $J = 15.2$, 1H), 4.17 (d, $J = 15.2$, 1H), 3.81 (m, 3H), 3.20 (m, 3H); MS (ESI $^+$) m/z 401.11 [M + H] $^+$.

Characterization of Compound 14{12,4}. $^1\text{H NMR}$ (300 MHz, CDCl_3) 8.01 (bs, 1H), 7.39–6.83 (m, 14H), 5.48 (d, $J = 3.8$, 1H), 4.66 (bs, 1H), 4.18 (m, 2H), 3.61 (m, 2H), 3.21–2.90 (m, 6H), 1.47 (m, 2H), 1.25 (m, 6H), 0.85 (m, 3H); MS (ESI $^+$) m/z 535.13 [M + H] $^+$, m/z 557.29 [M + Na] $^+$.

Characterization of Compound 15{4,4}. $^1\text{H NMR}$ (500 MHz, CDCl_3) 7.75 (m, 1H), 7.54 (m, 2H), 7.46 (m, 3H), 6.88 (m, 1H), 6.74–6.61 (m, 5H), 6.47 (s, 1H), 5.78 (s, 1H), 5.06 (s, 1H), 4.82 (d, $J = 14.9$, 1H), 4.13 (d, $J = 15.1$, 1H), 3.80 (dd, $J = 12.2$, 4.1, 1H), 3.18 (m, 3H); MS (ESI $^+$) m/z 459.87 [M + H] $^+$.

Characterization of Compound 15{7,4}. $^1\text{H NMR}$ (500 MHz, CDCl_3) 7.73 (m, 1H), 7.53 (m, 2H), 7.39 (m, 3H), 6.79 (m, 3H), 6.69 (d, $J = 8.5$, 2H), 6.60 (s, 1H), 6.53 (s, 1H), 5.70 (s, 1H), 4.93 (d, $J = 4.7$, 1H), 3.73 (m, 5H), 3.26 (m, 1H), 3.10 (m, 3H), 2.58 (m, 2H); MS (ESI $^+$) m/z 485.93 [M + H] $^+$.

Characterization of Compound 16{7,1}. $^1\text{H NMR}$ (500 MHz, CDCl_3) 7.26 (m, 5H), 6.81 (d, $J = 8.4$, 2H), 6.70 (d, $J = 8.3$, 2H), 6.58 (s, 1H), 6.55 (s, 1H), 5.78 (t, $J = 5.3$, 1H), 5.21 (d, $J = 5.2$, 1H), 4.74 (d, $J = 5.4$, 1H), 4.39 (d, $J = 5.4$, 2H), 3.76 (m, 4H), 3.60 (m, 1H), 3.14 (m, 2H), 2.94 (m, 2H), 2.58 (m, 2H); MS (ESI $^+$) m/z 488.85 [M + H] $^+$.

Characterization of Compound 16{7,2}. $^1\text{H NMR}$ (500 MHz, CDCl_3) 6.80 (d, $J = 8.6$, 2H), 6.70 (d, $J = 8.5$, 2H), 6.58 (s, 1H), 6.56 (s, 1H), 5.89 (m, 1H), 5.86 (m, 1H), 5.20 (s, 1H), 5.13 (d, $J = 15.9$, 1H), 5.06 (d, $J = 10.2$, 1H), 4.81 (s, 1H), 3.76 (m, 6H), 3.60 (m, 1H), 3.19 (m, 1H), 3.12 (m, 1H), 3.01 (d, $J = 11.5$, 1H), 2.89 (d, $J = 14.9$, 1H), 2.58 (m, 2H); MS (ESI $^+$) m/z 438.88 [M + H] $^+$.

Characterization of Compound 16{12,4}. $^1\text{H NMR}$ (500 MHz, CDCl_3) 7.14 (m, 6H), 7.06 (d, $J = 7.1$, 2H), 7.00 (d, $J = 7.8$, 2H), 6.49 (s, 1H), 6.33 (s, 1H), 6.18 (bt, 1H), 5.04 (s, 1H), 4.78 (d, $J = 5.6$, 1H), 4.15 (t, $J = 7.2$, 1H), 3.98 (m, 3H), 3.69 (m, 1H), 3.50 (dd, $J = 11.3$, 4.8, 1H), 3.06 (m, 8H), 2.85 (d, $J = 11.0$, 1H), 2.78 (d, $J = 14.8$, 1H), 1.47 (m, 2H), 1.25 (m, 6H), 0.87 (m, 3H); MS (ESI $^+$) m/z 528.95 [M + H] $^+$.

Characterization of Compound 16{1,7}. $^1\text{H NMR}$ (500 MHz, $\text{DMSO}-d_6$) 8.50 (t, $J = 10.7$, 1H), 7.48 (d, $J = 8.8$, 2H), 7.18 (d, $J = 8.9$, 2H), 6.68 (s, 1H), 6.58 (s, 1H), 5.43

(s, 1H), 5.11 (d, $J = 5.6$, 1H), 3.86 (dd, $J = 11.8, 4.2$, 1H), 3.22 (m, 3H), 2.90 (m, 2H), 1.77 (m, 1H), 0.71 (d, $J = 6.9$, 3H), 0.56 (d, $J = 6.9$, 3H); MS (ESI⁺) m/z 430.82 [M + H]⁺.

Acknowledgment. This work was supported by (1) Grant CBM2-B113-001-1-0-0 from the Center for Biological Modulators of the 21st Century Frontier R&D Program, the ministry of Science and Technology, Korea (MOST); (2) the Korean Science and Engineering Foundation (KOSEF); and (3) MarineBio21, Ministry of Maritime Affairs and Fisheries, Korea (MOMAF). S.-C.L. is grateful to the Seoul Science Fellowship. The authors thank Mr. Ji-Hyun Jung and Dr. Sung Kwang Lee for their technical assistance in the NMR and chemoinformatics studies, respectively.

Supporting Information Available. Copies of ¹H NMR, COSY, and mass spectra for the representative library members. Complete NMR study (COSY, HBMC, HSQC, and NOESY) to confirm the regioselectivity and diastereoselectivity with compound **16**{10,1}; this was associated with data analysis. LC/MS spectra (PDA detector) of 90 representative final library compounds without further purification. This material is available free of charge via the Internet at <http://pubs.acs.org>.

References and Notes

- (1) (a) Wessjohann, L. A. *Curr. Opin. Chem. Biol.* **2000**, *4*, 303. (b) Tan, D. S. *Nat. Chem. Biol.* **2005**, *1*, 74.
- (2) Wipf, P. *Pharm. News* **2002**, *9*, 157.
- (3) Boldi, A. M. *Curr. Opin. Chem. Biol.* **2004**, *8*, 281.
- (4) Clardy, J.; Walsh, C. *Nature* **2004**, *432*, 829.
- (5) Newman, D. J.; Cragg, G. M.; Snader, K. M. *J. Nat. Prod.* **2003**, *66*, 1022.
- (6) González, J. F.; Cuesta, E.; Avendano, C. *Tetrahedron* **2004**, *60*, 6319.
- (7) Chan, C.; Heid, R.; Zheng, S.; Guo, J.; Zhou, B.; Furuuchi, T.; Danishefsky, S. J. *J. Am. Chem. Soc.* **2005**, *127*, 4596.
- (8) Myers, A. G.; Kung, D. W. *J. Am. Chem. Soc.* **1999**, *121*, 10828.
- (9) Myers, A. G.; Lanman, B. A. *J. Am. Chem. Soc.* **2002**, *124*, 12969.
- (10) Peng, Y.; Tao, W.; Fuxiang, Y.; Cook, J. M. *Tetrahedron Lett.* **1997**, *38*, 6819.
- (11) For a review on the solid-phase Pictet–Spengler reaction, see: Nielsen, T. E.; Diness, F.; Meldal, M. *Curr. Opin. Drug Discovery Dev.* **2003**, *6*, 801.
- (12) Orain, D.; Canova, R.; Dattilo, M.; Klöppner, R. D.; Koch, D.; Giger, R. *Synlett* **2002**, *9*, 1443
- (13) (a) Nielsen, T. E.; Meldal, M. *J. Comb. Chem.* **2005**, *7*, 599. (b) Danieli, B.; Giovannelli, P.; Lesma, G.; Passarella, D.; Sacchetti, A.; Silvani, A. *J. Comb. Chem.* **2005**, *7*, 458. (c) Kundu, B.; Sawart, D.; Chhabra, R. *J. Comb. Chem.* **2005**, *7*, 317. (d) Veerman, J. J. N.; Bon, R. S.; Hue, B. T. B.; Girones, D.; Rutjes, F. P. J. T.; Maarseveen, J. H.; Hiemstra, H. *J. Org. Chem.* **2003**, *68*, 4486.
- (14) (a) Mohan, R.; Chou, Y.-L.; Morrissey, M. M. *Tetrahedron Lett.* **1996**, *37*, 3963. (b) Dressman, B. A.; Spangle, L. A.; Kaldor, S. W. *Tetrahedron Lett.* **1996**, *37*, 937. (c) Yang, L.; Guo, L. *Tetrahedron Lett.* **1996**, *37*, 5041. (d) Mayer, J. P.; Bankaitis-Davis, D.; Zhang, J.; Beaton, G.; Bjergarde, K.; Andersen, C. M.; Goodman, B. A.; Herrera, C. J. *Tetrahedron Lett.* **1996**, *37*, 5633.
- (15) Tang, Y.-F.; Liu, Z.-Z.; Chen, S.-Z. *Tetrahedron Lett.* **2003**, *44*, 7091.
- (16) Corey, E. J.; Gin, D. Y.; Kania, R. S. *J. Am. Chem. Soc.* **1996**, *118*, 9202.
- (17) (a) Maarseveen, S. H.; Mulders, S. J. E.; Aben, R. W. M.; Kruse, C. G.; Scheeren, H. W. *Tetrahedron* **1995**, *51*, 4841. (b) Ungemach, F.; Cook, J. M. *Heterocycles* **1978**, *9*, 1089.
- (18) (a) Vojkovsky, T.; Weichsel, A.; Pátek, M. *J. Org. Chem.* **1998**, *63*, 3162. (b) Eguchi, M.; Lee, M. S.; Nakanishi, H.; Stasiak, M.; Lovell, S.; Kahn, M. *J. Am. Chem. Soc.* **1999**, *121*, 12204.

CC0501054